The International Journal of Advanced Manufacturing Technology (2024) 130:1451–1463
https://doi.org/10.1007/s00170-023-12467-x

ORIGINAL ARTICLE

Application and evaluation of classic and demand oriented cooling strategies in context of machine tools

Eric Wenkler[1,2] · Christoph Steiert[1] · Steffen Ihlenfeldt[1,2] · Jürgen Weber[1]

Received: 23 June 2023 / Accepted: 24 September 2023 / Published online: 11 December 2023

Abstract
Energy consumption is an important factor in the operation of machine tools. Recent studies showed that in average, 1/5 of the machine tools total energy demand is caused by internal cooling systems. The continually rising performance of machine tools, together with the importance of thermal stability, reasons the requirement for demand oriented cooling approaches, which could significantly reduce the energy consumption for internal machine cooling. This study applied classic and demand oriented cooling strategies on a machine tool frame, which is one of the most complex machine tool components from a thermal point of view. The demand oriented cooling is based on volume flow control and can either be configured close to the environmental temperature or close to the thermal steady state, which can be obtained by loss forecast in combination with an FE model or measurement. The impact of the strategies on the thermal reaction as well as the energy consumption is compared, showing a significant reduction of energy demand without significant impairment of the thermal stability.

Keywords Machine tool · Temperature · Cooling · Energy efficiency

1 Introduction

Machine tools are the core manufacturing system for the accurate machining of metal parts as well as plastic components, as required, for example, in the automotive or aerospace sector. To raise their productivity and with that the economic benefit for the manufacturers, drive powers and axis speeds have continually increased. This increase caused in addition an unintended increase of losses, the occurring heat spreads within the machine tool. Since heat leads to a thermo-elastic deformation that impairs the manufacturing accuracy, the increase of performance must always consider a potential decrease in accuracy [1].

To overcome this limitation, high effort is put by industry and research into controlling thermo-elastic deformations, which will be described in more detail in Sect. 2. One of the most applied solutions is the integration of cooling systems, which are providing tempered fluid in lossy assemblies [2]. With this approach, the generated heat can be transported out of the machine tool by the fluid, which maintains the initial machine temperature. Nowadays, cooling systems are causing approximately 1/5 of the complete machine tools energy demand, with an increasing tendency. This collides with current ambitions regarding energy efficiency and sustainable manufacturing. A grate potential is seen in decentralised cooling systems for reducing the energy consumption of the machine tool, while maintaining its temperature [2, 3].

The quantification of this potential is in the focus of this paper. Herefore, multiple control approaches for a decentralised cooling system are applied and evaluated to quantify their impact on the thermal and energetic behaviour. A machine tool frame was chosen as research object and demonstrator, since it is one of the most complex machine tool components, from a thermal point of view, according to high heat capacities and low conductivity, which is challeng-

Eric Wenkler and Christoph Steiert equally contributed to this work.

✉ Eric Wenkler
eric.wenkler@tu-dresden.de

Christoph Steiert
christoph.steiert@tu-dresden.de

Steffen Ihlenfeldt
steffen.ihlenfeldt@tu-dresden.de

Jürgen Weber
fluidtronik@tu-dresden.de

[1] Institute for Mechatronic Engineering, TU Dresden, HelmholtzstraSSe 7a, Dresden 01069, Germany

[2] Institute for Machine Tools and Forming Technology IWU, Fraunhofer, Nöthnitzer Str. 44, Dresden 01187, Germany

ing for a controlled heat removal. Therefore, the approach should be transferable to other machine tool components with less heat capacities and greater losses, as for example a main spindle.

2 State of the art

The industry sector holds a significant share of a country's total energy demand, especially in industrialised countries. For example, in Germany, 31% of the total energy demand is required for the producing industry, from which 22% are caused by metal working [4]. Since machine tools are the most used tool for machining of metals, they have a significant impact on the resulting 7% of the energy consumption in Germany.

The effective usage of machine tools is therefore of high priority. One of the most limiting problems during machining are thermal issues, since the thermo-elastic deformation significantly influences the positioning accuracy of the machine tool and, with that, the geometric accuracy of the produced part. Studies show that more than half of all errors are reasoned out of thermal issues during manufacturing [5].

Approaches for the minimization of thermo-elastic deformations can be grouped into three categories, according to [6]:

- Heat flow control into the machine tool
- Constructive optimisations to reduce the sensitivity to heat flows
- Control-based compensation of thermo-elastic displacements

One of the most common approaches is the integration of heat sinks, which allow a controlled heat removal from the machine tool. Commonly, such heat sinks are achieved by integrating fluid channels close to lossy assemblies that are flooded with tempered fluid. With this, the majority of the generated heat can be transferred out of the machine, which significantly reduces thermo-elastic deformations. According to multiple energy consumption studies, actual cooling systems demand approximately 1/5 of the total machine tool power consumption [7–9]. A big potential is seen in demand oriented cooling [2, 10], which reasons this investigation on quantifying this potential.

Another major research field are constructive optimizations, which are mainly achieved by the integration of thermally resistant materials, on which a good overview on relevant materials is given by Möhring et al. [11]. It is also common to do thermal simulations of assemblies or complete machine tools to analyse the thermal behaviour and optimise geometry or subcomponents to reduce their thermal sensitivity [12]. One recent example for a constructive optimisation is the integration of assemblies based on phase changing materials. Voigt et al. [13] showed that with the integration of phase changing materials in lossy assemblies, thermal changes can be reduced. These materials absorb the heat without increasing temperature but change their phase, e.g. from solid to liquid. With this method, heat peaks can be damped.

The third group summarises control-based approaches for correction of thermo-elastic deformations. The key idea is to estimate the thermo-elastic displacement and compensate it by adding an offset to the tool centre point via the machine control. With this approach, no additional energy is required for correction of the position error, making it an interesting approach for ecological manufacturing. The accurate estimation of thermo-elastic displacements is the major challenge that comes with huge modelling and parametrisation effort usually done with finite element (FE) models [5]. To overcome the effort required for FE models, alternative approaches are researched, which may substitute FE models.

Comparable results can be achieved with alternative model approaches. Su et al. [14] used a finite volume model for a hydrostatic spindle, which is better suited for cross-domain computations like thermo-elastic simulation coupled to a computational fluid dynamics model. Thiem et al. [15] showed how structure models can be created and used for achieving an online capable thermal model. Naumann et al. [16] created and applied characteristic diagrams for thermo-elastic predictions. These three examples show the relevance of reliable and fast thermo-elastic computations, which are from major interest for a practical application of control-based approaches.

Conclusively, it can be stated that the importance of controlling the thermo-elastic machine tool behaviour is well known. While industry mainly applies cooling systems in combination with a thermal resistant machine setup, research focusses on the model-based prediction and correction of thermo-elastic errors. Since model-based corrections are still struggling with complexity, generalisation and real time capability, the energy demanding cooling systems will stay the best-practice approach within the next decades. Therefore, their improvement is of high importance of the metal working sector.

3 Demonstrator

The application and evaluation of demanded cooling requires multiple controllable cooling circuits and integrated temperature sensors, which is not common for current machine tools. Therefore, a machine tool frame was created in cooperation with FRAMAG and Hydac, which satisfies these require-

ments. The machine tool frame was chosen as one of the most complex machine tool components, according to its major heat capacity and low conductivity. These properties are challenging for the long-term thermal stabilisation, which is essential in series and mass production.

The demonstrator can be divided into two main components: first, the machine tool frame, which is described in Sect. 3.1, and second, the fluid system, which will be described in Sect. 3.2.

3.1 Machine tool frame

The machine tool frame is U-shaped and made of Hydropol® by the company FRAMAG. The design was developed in consultation between research and industry to allow demanded cooling and is derived from a milling machine tool with parallel kinematics. Figure 1a gives a general impression of the raw tool frame and connected peripherals. It has a width of 1.4m, a depth of 2 m, a height of 1.6 m, and a weight of 8200 kg. Inside a steel case, it is cast with Hydropol®. Table 1 summarises the thermal and mechanical properties of Hydropol® in comparison to steel. Included into the machine tool frame are 30 calibrated PT100 temperature sensors. In addition, ten PT100 temperature sensors are placed around the machine tool frame, one at the surface of a heating mat, eight to measure the ambient temperature at all corners and one close to the cooling systems fan. The positions are given in Fig. 1c.

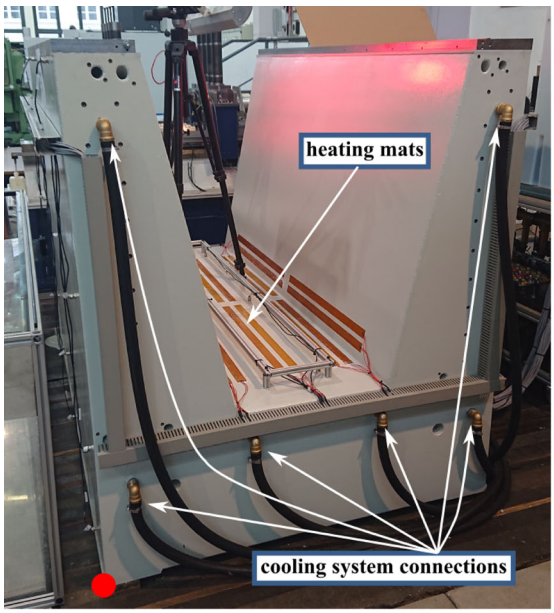

(a) Raw machine tool frame

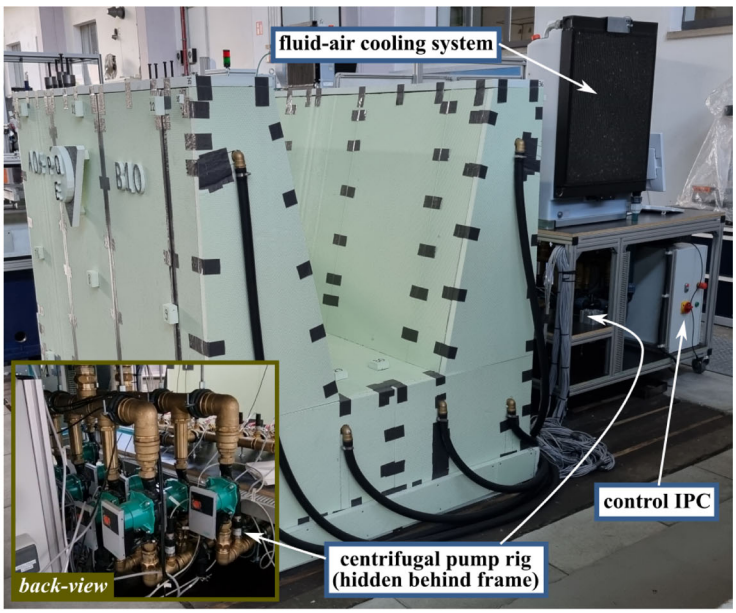

(b) Insulated demonstrator (test-setup)

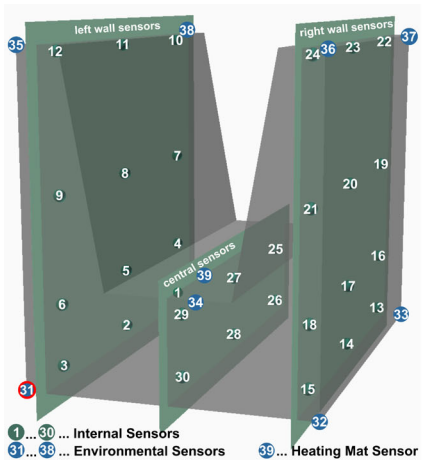

(c) Temperature sensors and groups

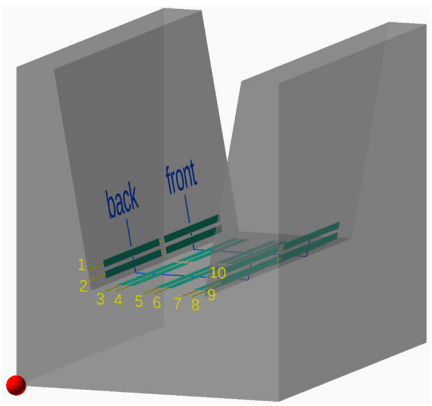

(d) Heating mats

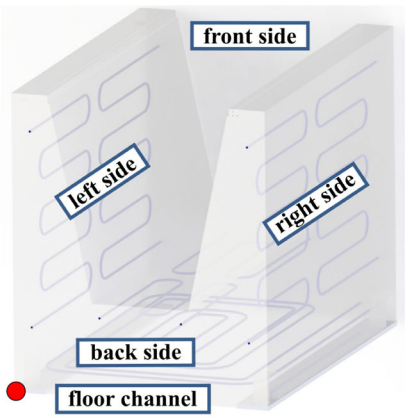

(e) Cooling channels

Fig. 1 Demonstrator characteristics

Table 1 Properties of installed materials according to [17]

Property	Steel	Hydropol®	Unit
E-module	210.000	37.000	MPa
Coefficient of expansion	12e-6	10e-6	K^{-1}
Thermal conductivity	60	6.2	$Wm^{-1}K^{-1}$
Specific heat capacity	435	980	$Jkg^{-1}K^{-1}$
Density	7850	2450	kgm^{-3}
Poisson's ratio	0.3	0.2	-

The frame structure has seven integrated tempering channels that are shown in Fig. 1e, which are used to remove heat and thus cool the machine frame. One channel is located at the ground of the machine frame and formed as a spiral, similar to underfloor heating systems. This channel is named "floor channel" and has the aim to decouple the machine frame from the foundation of the production facility. Two channels are placed on the right and left sides of the central area, where significant heat is assumed, caused by, for example, drive losses or hot chips. Therefore, the channels are called "chip channel right" or "chip channel left". The last four channels are located in the sides of the machine frame and are named "side channel" appended by "front" or "back" and "left" or "right" to describe their location. The length of all tempering channels is given in Table 2. The inner diameter of the channels is 0.024 m, and the outer diameter is 0.028 m.

Furthermore, the machine tool is equipped with 20 heating mats. Each of the mats is controllable and has a heating power of 45 W, allowing a maximum heat introduction of 900 W. Figure 1d shows the position of the heat mats and their numbering.

Preceding measures showed that the not air-conditioned hall temperature behaves unpredictable. Figure 2 shows the measured environmental temperature during summer and winter. Especially during summer, when high temperatures occur, the hall gate gets opened at shift start and closed at shift end, which leads to major changes over the day cycle. These changes reduce at the weekend, where the hall gate stays closed. Similar effects can be observed in winter, where the

Table 2 Length of the tempering channels

Channel name	Length
Floor channel	18.97m
Chip channel right	3.66m
Chip channel left	3.66m
Side channel front right	7.10m
Side channel front left	7.10m
Side channel back right	7.10m
Side channel back left	7.10m

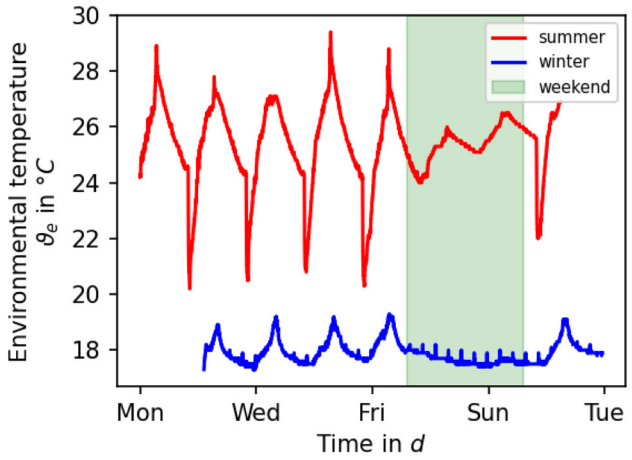

Fig. 2 Seasonal impact on the environmental temperature inside the hall

temperature stabilizes at the weekend according to an inactive hall heating. Since precision machining is not done under such conditions, the machine frame was put in insulation, as shown in Fig. 1b, to decouple the machine frame from the environment. A further benefit of the insulation is the better observability of the cooling system influence, according to the reduction of side effects. The insulation is made of Styrodur® and has a thickness of 0.030 m.

3.2 Fluid system

The fluid system supplies the machine tool frame with tempered fluid and has ten centrifugal pumps that can separately supply 10 cooling circuits. Figure 3 shows a schematic description of the fluid system. The pump speed can be set constant or controlled to achieve a stable volume flow. To observe the thermal condition of the fluid, different sensors are integrated. Each of the ten available circuits has a volume flow, temperature and pressure sensor in the fluid inlet. In addition, each fluid return is equipped with a temperature sensor and one further pressure sensor in the merger of the ten returns.

The fluid tempering is achieved by a fluid-air cooling system named FLKS-5EC3, obtained from the company Hydac. Its heat removal capacity depends on two major factors, which are the temperature gradient between fluid and environment $\Delta\vartheta_{f\to e}$ and the fan rotational speed n. At maximum fan speed n, the cooling system reaches its maximum heat transfer of 0.98 kWK^{-1}.

3.3 Control design

The control is a programmable logical controller (PLC) using Beckhoff components and was programmed to provide an easy interface for heating mat control, case dependent actu-

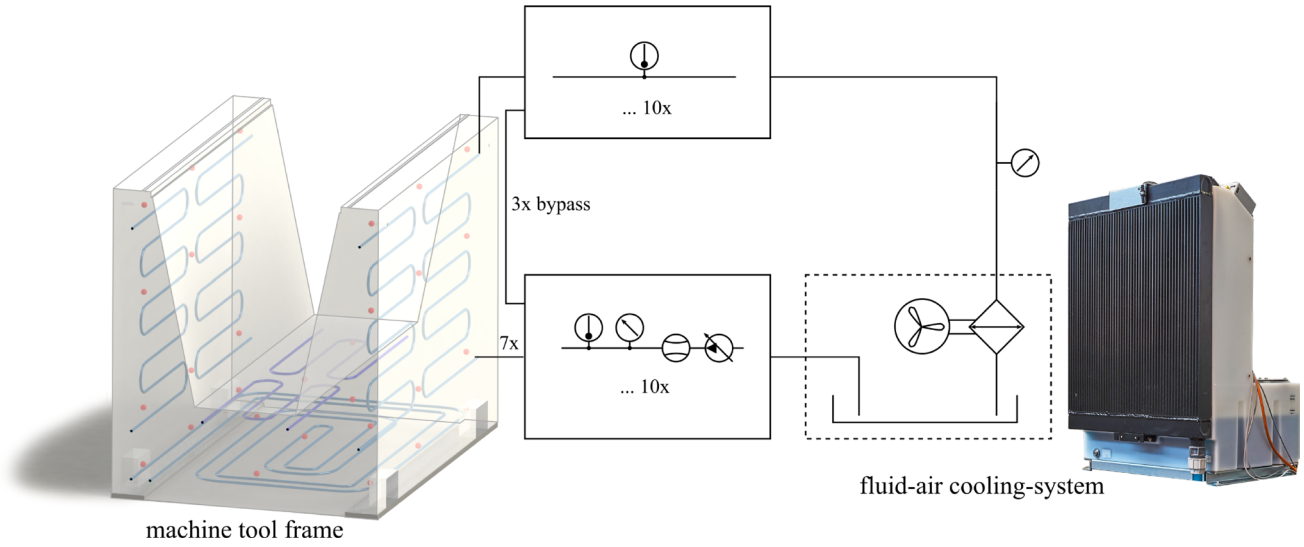

Fig. 3 Schematic description of the fluid system

ator control and data capture. It supports repetitive task execution used for long-term measures and handles:

- Internal sensor data collection and structuring
- Actuator control
  - Heating mats, which are pulse width modulated (PWM) to achieve a dynamic heat introduction
  - Pumps, also with static volume flow or PI controlled, depending on temperatures
  - Fan, which can either be operated with constant rotational speed or PI controlled, to maintain a specific fluid temperature
- Python based IO-Interfaces using Beckhoff's Automation Device Specification (ADS)
  - Heating mat interface which transfers target activities from local CSV files to the PLC
  - Data acquisition interface which cyclically captures actual values from the PLC

4 Control strategies for decentralised cooling

This section describes the four considered cooling strategies used for evaluating their thermal impact on the machine tool frame and the energetic impact on the cooling system. The strategies are ordered by complexity and will be described separately in the following sections. Figure 4 gives a schematic overview for each considered cooling strategy.

4.1 Constant cooling (CC)

The method of constant cooling is widely spread in production systems, especially in machine tools. Here, a constant speed drive pump delivers a static volume flow through all channels of the system. The consumed power of the pump is therefore stable through the whole running phase. The fan is PI controlled to maintain a stable offset of $\Delta\vartheta = 1\text{K}$ between environment and fluid temperature. With this approach, the fan does not have to rotate at maximum speed, which leads to a slight energy saving in the cooling system. The approach is comparable to uncontrolled heat exchangers, which work with a static fan speed. Advantages of this method are low efforts regarding the implemented control strategies and affordable components, since no frequency converter is required for the pumps.

Nowadays, such approaches are not common, since environmental dynamics are directly transferred into the fluid. Furthermore, this approach provides insufficient capability to react to changes in bounding conditions. Therefore, it was only considered showing the disadvantages of a bad-tempered fluid.

4.2 Constant volume flow with variable cooling fan speed (CV)

To overcome the disadvantages that come with the cooling strategy described in Sect. 4.1, the temperature of the fluid has to be controlled. This can be achieved by controlling the fan speed to maintain a static fluid temperature, which requires a small thermal offset between environment and fluid $\Delta\vartheta_{f\to e}$. The target fluid temperature ϑ_f should consider the mean

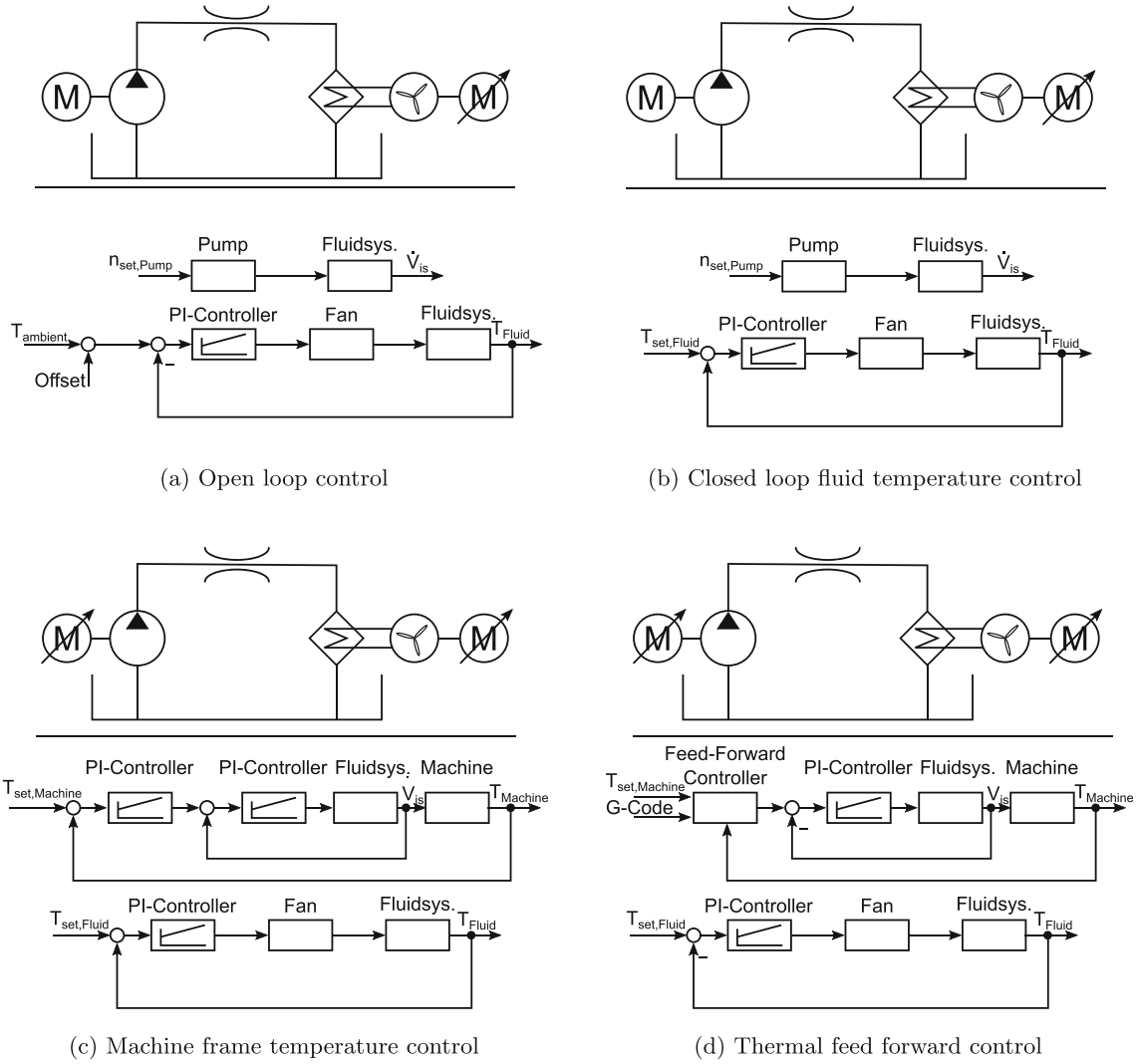

(a) Open loop control

(b) Closed loop fluid temperature control

(c) Machine frame temperature control

(d) Thermal feed forward control

Fig. 4 Schematic description of the four cooling strategies

environmental temperature $\overline{\vartheta_e}$ of the recent days, according to (1):

$$\vartheta_f = \overline{\vartheta_e} + \Delta\vartheta_{f\to e} \tag{1}$$

The offset $\Delta\vartheta_{f\to e}$ should be small enough to keep the fluid cold and achieve a maximal possible temperature gradient between fluid and machine tool frame temperatures, but also high enough to overcome environmental changes, since a convective heat transport to the environment is only possible if the environment is colder than the fluid. This disadvantage with convective heat exchanges reasons the wide usage of the energetic, inefficient compressor-based chillers.

With this strategy, two positive properties are introduced. First, with a controllable flow temperature, the environmental conditions have a smaller influence on the fluid system, and second, the fan consumes only power if a cooling of the fluid is required.

This cooling strategy represents the state of the art of actual cooling systems and is therefore used as reference for comparing cooling strategies in later sections.

4.3 Variable volume flow with variable cooling fan speed (VV)

The third cooling strategy introduces a dynamic volume flow $\dot{V}_i$, while the fan is still controlled to maintain a stable fluid temperature. The pump activity gets controlled to adjust the volume flow in order to maintain specific temperatures in the machine tool frame. Herefore, the inner thermal sensors (Fig. 1c) are assigned to the closest cooling channel (Fig. 1e), and the mean temperature of this sensor group is used as set point for the single pump control. This approach requires two control offsets: one between fluid and environment $\Delta\vartheta_{f\to e}$ to control the fan, and one between the tool frame and the

environment $\Delta\vartheta_{tf\to e}$ to achieve a heat flow between tool frame and fluid. The condition in (2) has to be satisfied in order to achieve a heat flow from the demonstrator, over the fluid, to the environment. The control offsets have to be small to ensure a heat removal, even if less heat is generated by the process.

$$(\vartheta_e < \vartheta_f < \vartheta_{tf}) \rightarrow (\Delta\vartheta_{f\to e} < \Delta\vartheta_{tf\to e}) \tag{2}$$

4.4 Thermal feed-forward control (VV+)

The last approach is an extension of the volume flow controlled cooling approach in Sect. 4.3. The previews cooling strategy used small differences in the control offsets to ensure the possibility of cooling, even at times when less heat reaches the demonstrator. By consideration of task caused power losses, a forecast of the uncooled thermal steady state is possible, which allows the determination of heterogeneous thermal set points, close to the uncooled steady state. With this, the majority of generated heat remains in the demonstrator, and the cooling system is only used for temporal stabilisation of the heterogeneous temperature, which has a significant impact on the power demand of the pumps.

The uncooled thermal steady state can either be measured with a deactivated cooling system or predicted by simulation. Within previews research is shown that task-specific losses are predictable [18] and can be used as boundary conditions in transient FE models for predicting the thermal behaviour [19]. The opportunity to forecast the task-specific thermal behaviour is especially interesting for low batch manufacturing, where the measurement of the thermal steady state would cause to high costs.

5 Application

5.1 Thermal load scenario

Machine tools and their assemblies, such as the considered machine bed, are exposed to strongly fluctuating thermal loads, which are caused by lossy assemblies like the motor or bearings and vary significantly with the machining process. Therefore, it is important to apply a realistic thermal load scenario to compare the cooling strategies under realistic conditions. Such conditions can be obtained by defining a typical manufacturing task and perform a power loss forecast [18]. For this purpose, a typical aerospace component was designed, which are usually large, light and machining-intensive, with removal rates above 80%. Figure 5a shows the prepared component including its manufacturing steps for the first clamping, which is typical for support structures in planes, rockets or satellites. Its main dimensions are $514 \times 310 \times 150$ mm, and the machining time is ≈ 4.5 h.

The G-Code, obtained from the process planning, was passed to a loss prediction strategy to obtain realistic power losses. Since the machine tool frame is without mechanical actuators, an x-axis was assumed to be mounted in the centre of the frame, and the heating mats were used to mimic axis-specific losses of the assumed axis, as shown in Fig. 5b. Further details to the loss prediction, transformation and imitation via heating mats can be obtained from [19].

5.2 Measurement setup

The physical properties together with the great dimensions of the machine tool basis lead to a very slow thermal response. Initial measures showed that, depending on the cooling strat-

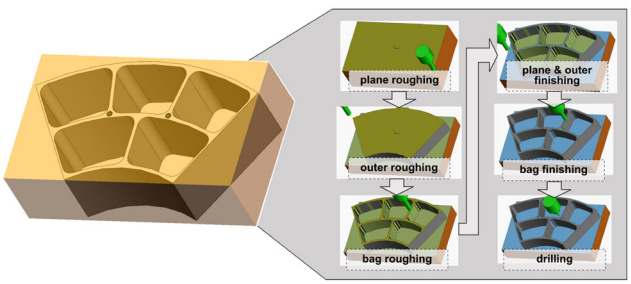

(a) Reference process for determination of realistic thermal loads

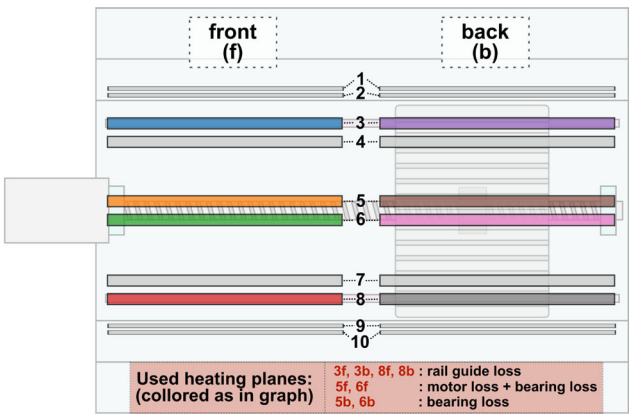

(b) Imitation of axis specific power losses via heating mats

Fig. 5 Application of realistic thermal loads to the demonstrator according to [19]

egy, the machine tool frame requires 1 to 3 days until it reaches steady state. Therefore, it is necessary to perform long-term measures to compare the cooling strategies with each other.

A further significant influence is the change in environmental temperature. Since the machine hall is not air-conditioned and therefore responds to weather changes, there is a high risk of obtaining unexpected thermal influences, as indicated by Fig. 2. Multiple measures had to be repeated according to unexpected weather changes, like a change from cloudy days to sunny days or a temperature increase or drop by >5 K, which directly influences the environmental temperature inside the hall and made the comparison of the cooling approaches impossible.

The measures were taken from 1 week up to 2 weeks, depending on environmental conditions. Since the process itself takes only about 4.5 h, the process was executed in a loop with 10 min pauses in between, which are a typical time for a work piece and tool change in industry. The measures can therefore be compared to a typical series or mass production. The following 61 sensor information were captured each 60 s for evaluation purposes, which is a sufficient interval according to the slow response of the demonstrator:

- 9x Environmental temperature $\vec{\vartheta}_e$
- 30x Machine tool frame temperature $\vec{\vartheta}_s$
- 7x Fluid inlet temperature $\vec{\vartheta}_{fi}$
- 7x Fluid outlet temperature $\vec{\vartheta}_{fo}$
- 7x Volume flow rate of fluid $\vec{\dot{V}}$
- Fluid Tank temperature ϑ_f

In addition, the fan speed n was captured beside the listed sensor information.

6 Evaluation

This section issues the comparison of the different cooling strategies together with their thermo-energetic impact on the machine tool frame. Initially, the thermal influence will be discussed in Sect. 6.1, followed by the energetic influence in Sect. 6.2.

It has to be mentioned that only a selected portion of the measured system behaviour will be considered in the following evaluations. The goal of introducing an evaluation area is to exclude uncomparable environmental influences to increase the comparability of the evaluations. Therefore, the evaluated area was manually set to exclude the following effects:

- The warm-up phase, since the initial temperature of the machine tool frame was not equal between the different measures, which directly affects the required time for warm-up where a thermal drift is unavoidable.
- Areas where the environment significantly exceeded the fluid temperature setpoint, since they are mainly caused by a bad setpoint definition or instable hall temperature and therefore not caused by the cooling strategy.

The used evaluation area will be indicated by a black horizontal within following figures that show the measured system behaviour (Figs. 6 and 8).

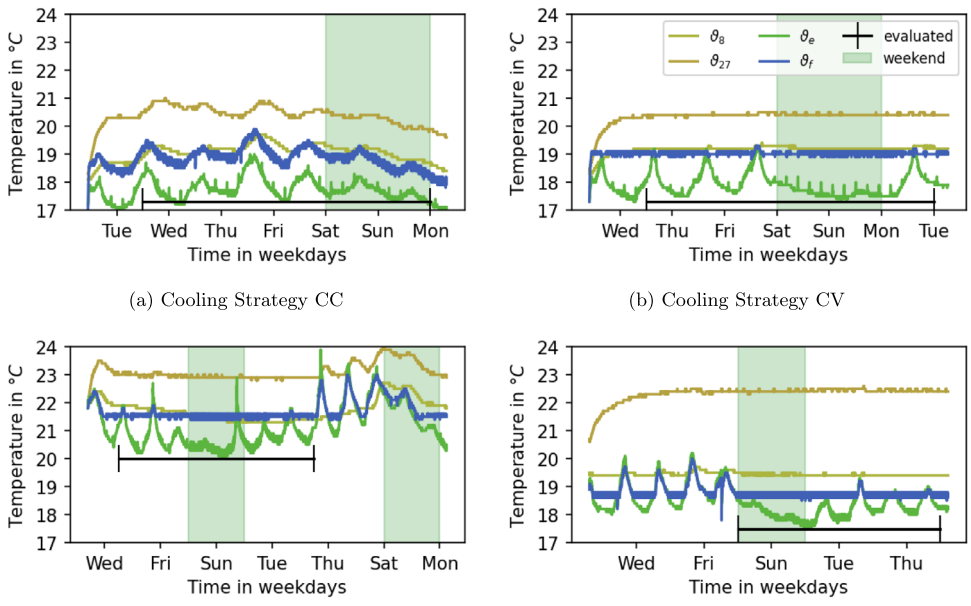

(a) Cooling Strategy CC

(b) Cooling Strategy CV

(c) Cooling Strategy VV

(d) Cooling Strategy VV+

Fig. 6 Impact of the cooling strategy on the thermal behaviour of selected internal Sensors (8 and 27, according to Fig. 1c), environment ϑ_e and fluid ϑ_f

6.1 Thermal evaluation

The main goal of machine tool tempering is the stabilisation of inner temperatures. Since thermal changes are the source for thermo-elastic deformations that directly influence the machining quality, their stabilisation is of high importance, especially in precision machining. The primary goal is a temporal stabilisation of inner temperatures to maintain a static thermo-elastic deformation during manufacturing. The secondary goal is often a homogeneous temperature field, as homogeneous temperatures do not cause heat flows and thus naturally remain thermally stable. Since the secondary goal cannot be achieved practically, warm-up cycles are a common approach for putting the machine in a thermal steady state. A general impression of the cooling strategies impact on the thermal behaviour is shown in Fig. 6, where selected sensor temperatures are shown together with the environmental and fluid temperature.

In order to characterise the temporal thermal stability, position-dependent statistical parameters were determined from the individual sensor temperatures. Herefore, the following notation is used: the sensor specific mean temperature $\mu_s = \overline{\vartheta}_s$ in °C, the sensor specific standard deviation σ_s in °C, the sensor specific variation range R_s in °C, the time dependent sensor temperature $\vartheta_s(t)$ in °C, the start and end time $t_0 \wedge t_1$ for the evaluated area in s (shown, e.g. in Fig. 6), the sampling rate t_s in s, and the sensor position index s.

$$\mu_s = \overline{\vartheta}_s = \frac{\sum_{t=t_0}^{t_1} \vartheta_s(t)}{\frac{t_1 - t_0}{t_s} + 1} \tag{3}$$

$$\sigma_s = \sqrt{\frac{\sum_{t=t_0}^{t_1} (\vartheta_s(t) - \mu_s)^2}{\frac{t_1 - t_0}{t_s} + 1}} \tag{4}$$

$$R_s = \max(\vartheta_s(t)) - \min(\vartheta_s(t)) \tag{5}$$

Figure 7 shows the detailed view of the position-dependent statistics with respect to the different cooling strategies of Sect. 4. In addition, the mean values for the statistics are represented by the dotted horizontal line.

The mean sensor temperature $\overline{\vartheta}_s$ shows a great offset for the cooling strategy VV. This is reasoned out of its application during summer, while the others were applied during winter, and is therefore no criteria for the comparison of the cooling strategies. The mean temperatures $\overline{\vartheta}_s$ may not be absolutely compared, but they allow a drawback on the homogeneity of the temperature field by calculating the mean μ_p and standard deviation σ_p of $\overline{\vartheta}_s$, according to (7):

$$\mu_p = \overline{\overline{\vartheta}_s} = \frac{\sum_{s=1}^{30} \overline{\vartheta}_s}{30} \tag{6}$$

$$\sigma_p = \sqrt{\frac{\sum_{s=1}^{30} (\overline{\vartheta}_s - \mu_p)^2}{30}} \tag{7}$$

A general impression for the temporal thermal stability can be obtained by averaging the standard deviation $\overline{\sigma_s}$ or alternatively the variation range $\overline{R_s}$, which both give an impression about the mean thermal change in the demonstrator. It has to be mentioned that this approach does

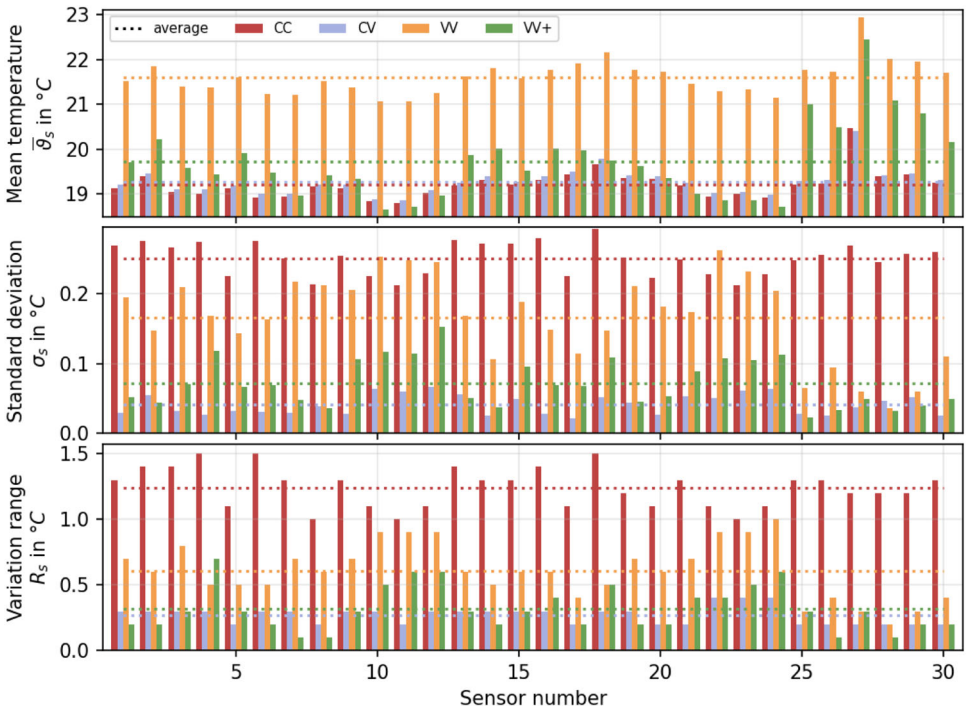

Fig. 7 Position-dependent statistics for the thermal behaviour with respect to the cooling strategy

Table 3 Characteristic values for comparing the thermal influence of the cooling approaches

Cooling strategy	Positional thermal deviation $[\sigma_p] = °C$	Mean thermal deviation $[\overline{\sigma_s}] = °C$	Mean thermal variation range $[\overline{R_s}] = °C$	Mean thermal offset $[\overline{\Delta\vartheta}] = °C$
CC	0.31	0.25	1.24	1.41
CV	0.29	0.04	0.27	1.36
VV	0.38	0.17	0.61	0.86
VV+	0.82	0.07	0.32	1.52

not consider sensor positions and is therefore only valid with a homogeneous sensor placement, as given in the demonstrator.

$$\overline{\sigma_s} = \frac{\sum_{s=1}^{30} \sigma_s}{30} \tag{8}$$

$$\overline{R_s} = \frac{\sum_{s=1}^{30} R_s}{30} \tag{9}$$

A further characteristic value is the mean thermal difference between demonstrator and environment $\overline{\Delta\vartheta}$, which correlates with the amount of heat remaining in the demonstrator. The higher this value, the lower the heat dissipated from the demonstrator, which should correlate with the energy efficiency.

$$\overline{\Delta\vartheta} = \mu_p - \overline{\vartheta_e} \tag{10}$$

Table 3 shows the characteristic values, according to (7) to (10), for each cooling strategy. All strategies lead to a small positional thermal deviation σ_p with ≈ 0.3°C, except strategy VV+ where it raises to ≈ 0.8°C, which is reasoned out of the higher position-dependent thermal set point values, compared to the other cooling strategies, meaning that the first three cooling approaches lead to a more homogeneous temperature field.

As previously argued, a temporally stable temperature field is the primary goal, which can be characterised by the mean thermal deviation $\overline{\sigma_s}$, according to (8). The central graph of Fig. 7 shows this criterion together with the mean value over all sensors. It can be seen that cooling strategies CC and VV are causing relatively high deviations compared to the strategies CV and VV+. In strategy CC, the major reason for this high value is the thermally unstable fluid, constantly flooding through the demonstrator, which pulls environmental dynamics into the tool frame. Strategy VV has also a relatively high value, which is estimated to come from the small thermal difference between environmental temperature and thermal set point value of the demonstrator, which decreases the heat removal capacity of the fluid system. Therefore, a further increase of the set point value could lead to an increase of temporal thermal stability for cooling approach VV. Comparable and small deviations could be achieved with the strategies CV and VV+.

The mean variation range $\overline{R_s}$, as defined in (9), is an alternative criterion that is comparable to the mean thermal deviation $\overline{\sigma_s}$, which instead only considers the global range of temperatures. Here, all approaches except CC could achieve relatively low values.

The last criterion is the thermal offset $\overline{\Delta\vartheta}$, which should generally grow with efficiency. Cooling strategy VV achieves the lowest value, which again indicates a too low set point value. The remaining strategies have a comparable value with ≈ 1.4 °C, leaded by cooling strategy VV+ which intentionally allows more heat at specific temperatures, which reasons the high value.

According to the preceding argumentation based on Table 3, the cooling strategies can be ranked from a thermal view point in the given order:

1. Strategy CV achieves the highest thermal stability ($\overline{\sigma_s}$), which reasons its use as state-of-the-art control approach for modern cooling systems.
2. Strategy VV+ achieves comparable results, by allowing higher positional deviations in temperature, to improve the effectiveness of the heat removal.
3. Strategy VV shows a significant $\overline{\sigma_s}$, but if compared by $\overline{R_s}$, thermal changes are in average within 0.6°C, which is still comparable.
4. Strategy CC shows the worst results, since the environmental dynamic of the environment is directly transferred to the demonstrator and therefore not used in modern machine tools.

6.2 Energetic evaluation

The energy demand is the major criterion, beside thermal criteria, to describe the effectiveness of the cooling system and should be as low as possible. Since the energy demand depends on the activity time of a system, the consideration of the power demand provides a more general criterion that allows a comparison of the cooling approaches.

Therefore, the power consumption of the fan P_f and the single pumps $P_{p,i}$ were computed by the measured activity,

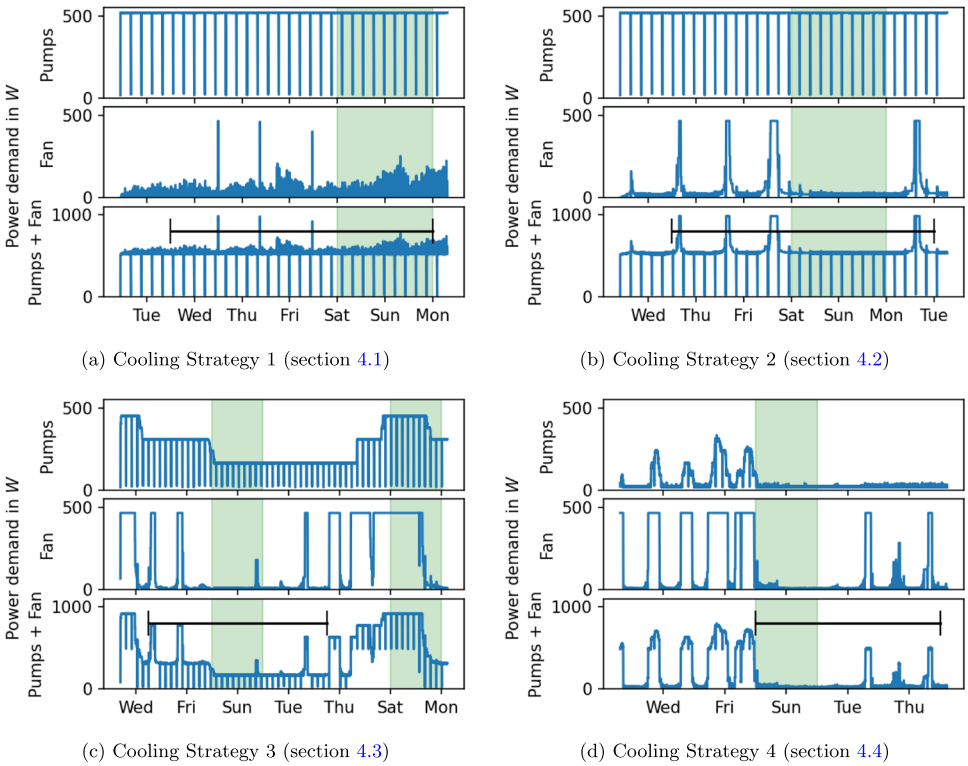

(a) Cooling Strategy 1 (section 4.1)

(b) Cooling Strategy 2 (section 4.2)

(c) Cooling Strategy 3 (section 4.3)

(d) Cooling Strategy 4 (section 4.4)

Fig. 8 Impact of the cooling strategy on the power demand

described by the rotational speed n or the volume flow $\dot{V}_i$. The fan was calibrated by a measurement of the power consumption at different rotational speeds, which is used for linear interpolation of the power demand. The power consumption of the pumps $P_{p.i}$ is also linear interpolated by preceding determination of the minimum power demand for creating a volume flow $P_0 = 4kW$ and the maximal flow at maximum power $\dot{V}(P = 75W) \approx 10Lmin^{-}1$.

Figure 8 shows the power demand for the different cooling strategies. For simplification, only the total power demand ($P_p = \sum_i P_{p.i}$) for all pumps is considered. Relative computations are shown in Table 4, with cooling strategy CV as reference, to compare the approaches to the state-of-the-art strategy.

Overall, it can be seen that the cooling approaches with uncontrolled pumps (CC and CV) are requiring much power, since they are permanently active, which reasons the majority of the total power demand. The difference of 5% is primarily reasoned out of the fan power demand, which is mainly influenced by the thermal offset between fluid and environment and therefore not directly a criterion for the cooling approach. Hence, the pump power demand P_p is the most relevant criteria for comparing the efficiency of the cooling approaches. Based on this criteria, no significant difference is visible in the first two cooling strategies (CC and CV).

With the usage of volume flow controlled approaches, in a manner of demanded cooling, the pumps energy consumption drops significantly. The main reason for the saving is that the pumps may adapt their activity to only provide the volume flow required to hold the desired thermal setpoint. Cooling approach VV achieved a pump power decreased by 58%, only because the pumps may now deactivate if no or lesser cooling is required. Since the savings correlate with

Table 4 Cooling strategy specific mean power demand, with strategy CV as reference

Cooling strategy	Mean fan power		Mean pump power		Mean total power	
	abs $[P_f] = \mathrm{W}$	rel $\frac{P_f}{P_{f.ref}}$	abs $[P_p] = \mathrm{W}$	rel $\frac{P_p}{P_{p.ref}}$	abs $[P] = \mathrm{W}$	rel. $\frac{P}{P_{ref}}$
CC	29.9	0.51	517.0	1.00	546.9	0.95
CV (ref)	59.0	1.00	516.7	1.00	575.7	1.00
VV	40.2	0.68	214.6	0.42	254.8	0.44
VV+	35.6	0.60	20.6	0.04	56.2	0.10

the remaining heat, cooling approach VV+ could achieve the highest energy saving with 96%.

From an energetic point of view, the demanded cooling holds therefore a significant potential for improving the energy efficiency of machine tools and components.

7 Conclusion and outlook

The paper compared four cooling strategies and their impact on thermal and energetic aspects. The first strategy showed the effects of a bad controlled fluid temperature, which is why this approach is outdated and no more used in industry. The second represents a state-of-the-art approach with a stabilised fluid temperature and permanently active pumps. Followed by, demand oriented cooling strategies that use volume flow controlled pumps, first with default thermal set points, followed by a task optimised one.

It could be shown that the strategy has a significant influence on thermal, especially energetic, criteria. Approach CC had the worst results, with major thermal changes and a high energy demand. The state-of-the-art approach achieved the best thermal stability but had the highest power demand. The demand oriented cooling approaches achieved a comparable thermal stability, especially approach VV+. The biggest benefit of demanded cooling shows in the energy demand of the cooling system. Only by applying the volume flow control, 56% of the energy can be saved, which increased with task optimised thermal set points up to 90%. If the fluid chilling is taken out of consideration, since its consumption is mainly caused by thermal dynamics in the environment and not the cooling approach, these savings grow even further (see Table 4).

Conclusively, it can be stated that demanded cooling approaches could achieve a significant benefit for increasing the cooling systems energy efficiency, especially if the growing energy demand of cooling systems is taken into account, which already now cause 1/5 of the machine tools total energy demand in average.

On the other hand, such approaches require the definition of thermal set points, which have to be chosen carefully. If wrongly defined, major thermal issues may arise, as visible outside the evaluation area in Figs. 6 and 8. Also, the heterogeneous temperature field, which reasons the energy saving of approach VV+, may get challenging during real manufacturing, since this requires a warm-up and a correction of the static thermo-elastic deformation that comes with the heterogene temperature.

Interesting approaches could go into the application of heat up concepts, where the machine is blocked after G-code selection, initiating a warm-up by using the cooling system, and unlock when the steady state is reached. In steady state, the raw part location and rotation can then be determined by tactile measurement and efficiently compensated with a static offset by the machine control. The applicability and potential challenges of such approaches could be promising directions for future research.

Acknowledgements The authors thank the companies Hydac Cooling GmbH and Framag Industrieanalgenbau GmbH for their support in relation to the demonstrator hardware.

Author Contributions All authors contributed to the study conception and design. Material preparation, data collection and analysis were performed by Eric Wenkler and Christoph Steiert. The first draft of the manuscript was written by Eric Wenkler in support from Christoph Steiert, and all authors commented on previous versions of the manuscript. All authors read and approved the final manuscript.

Funding Open Access funding enabled and organized by Projekt DEAL. The presented research activities are part of the projects A04 "Thermo-energetic description of fluid systems" and B10 "Thermal Precontrol" founded by the German Research Foundation (Project-ID 174223256 - TRR 96). The authors would like to thank the German Research Foundation (DFG) for the financial support of the research.

DFG Deutsche Forschungsgemeinschaft
German Research Foundation

The authors declare that no funds, grants, or other support were received during the preparation of this manuscript.

Declarations

Conflict of interest The authors declare no competing interests.

References

1. Grossmann K, Ott G (2015) Introduction. In: Grossmann K (ed) Thermo-energetic design of machine tools. Springer International Publishing, Switzerland, pp 1–11. isbn: 978-3-319-12625-8
2. Wegener K et al (2017) Fluid elements in machine tools. In: CIRP annals 66(2):611–634. https://doi.org/10.1016/j.cirp.2017.05.008
3. Shabi L (2020) Thermo-energetisch optimierte Fluid-Systeme für Werkzeugmaschinen. PhD thesis. Düren. isbn: 978-3-8440-7230-3
4. Statisitsches Bundesamt Destatis (2022) Umweltökonomische Gesamtrechnungen. Accessed: 13-June-2023. https://www.destatis.de/DE/ThemenGesellschaft-Umwelt/Umwelt/

UGR/energiefluesse-emissionen/Publikationen/Downloads/umweltnutzung-und-wirtschaft-energie-pdf-5850014.pdf
5. Mayr J et al (2012) Thermal issues in machine tools. In: CIRP annals 61(2):771–791. https://doi.org/10.1016/j.cirp.2012.05.008
6. Ramesh R, Mannan MA, Poo AN (2000) Error compensation in machine tools– a review. In: International journal of machine tools and manufacture 40(9):1257–1284. https://doi.org/10.1016/s0890-6955(00)00010-9
7. Denkena B et al (2011) Effiziente Fluidtechnik für Werkzeugmaschinen. In: Wt werkstattstechnik online 101(5):347–352. https://doi.org/10.37544/1436-4980-2011-5-347
8. Weber J, Weber J (2014) Thermoenergetic modelling of fluid power systems. In: Lecture notes in production engineering. Springer International Publishing, pp 49–59. https://doi.org/10.1007/978-3-319-12625-85
9. Weber J et al (2021) Investigation of the thermal and energetic behaviour and optimization towards smart fluid systems in machine tools. Procedia CIRP 99:80–85. https://doi.org/10.1016/j.procir.2021.03.014
10. Steiert C, Weber J, Weber J (2021) Examination of cooling systems in machine tools regarding system structure and control strategies. In: MM science journal 120–125. https://doi.org/10.17973/MMSJ.202172021060
11. Möhring HC et al (2015) Materials in machine tool structures. In: CIRP annals 64(2):725–748. https://doi.org/10.1016/j.cirp.2015.05.005
12. Jedrzejewski J et al (1990) Numerical optimization of thermal behaviour of machine tools. In: CIRP annals 39(1):379–382. https://doi.org/10.1016/s0007-8506(07)61077-4.
13. Voigt I et al (2019) Increased thermal inertia of ball screws by using phase change materials. Appl Thermal Eng 155:297–304. https://doi.org/10.1016/j.applthermaleng.2019.03.079
14. Su H et al (2014) Thermal analysis of the hydrostatic spindle system by the finite volume element method. In: The international journal of advanced manufacturing technology 71(9-12):1949–1959. https://doi.org/10.1007/s00170-014-5627-8
15. Thiem X et al (2023) Adaptive thermal model for structure model based correction. In: Lecture notes in production engineering. Springer International Publishing, pp 67–82. https://doi.org/10.1007/978-3-031-34486-26
16. Naumann C et al (2016) Characteristic diagram based correction algorithms for the thermo-elastic deformation of machine tools. Procedia CIRP 41:801–805. https://doi.org/10.1016/j.procir.2015.12.029
17. framag Industrieanlagen GmbH (2023) HYDROPOL®machine frames/machine beds. Accessed: 31-May-2023. url: https://www.framag.com/en/products/hydropolmachine-frames-4621.html
18. Wenkler et al E (2021) Part program dependent loss Forecast for estimating the thermal impact on machine tools. In: MM science journal, pp 4519–4525. https://doi.org/10.17973/MMSJ.202172021054
19. Wenkler E et al (2023) Analysing the impact of process dependent thermal loads on the prediction accuracy of thermal effects Effects in machine tool components. In: Lecture notes in production engineering. Springer International Publishing, pp 99–115. https://doi.org/10.1007/978-3-031-34486-28